Paradigm Academic Press
Journal of Innovations in Medical Research
ISSN 2788-7022
MAR. 2026 VOL.5, NO.1

Predictive Value of CCL3 Expression Levels for Therapeutic Response in Patients with Locally Advanced Cervical Cancer

Hang Chen[1] & Honelei Chen[2,3]

[1] Department of Biomedical Engineering, Wuhan University TaiKang Medical School (School of Basic Medical Sciences), Wuhan 430071, China

[2] Department of Pathology, School of Basic Medical Sciences, Wuhan University, Wuhan 430071, China

[3] Department of Pathology, Zhongnan Hospital of Wuhan University, Wuhan 430071, China

Correspondence: Honelei Chen, Department of Pathology, School of Basic Medical Sciences, Wuhan University, Wuhan 430071, China; Department of Pathology, Zhongnan Hospital of Wuhan University, Wuhan 430071, China.

doi:10.63593/JIMR.2788-7022.2026.03.001

Abstract

Rationale: Locally advanced cervical cancer (LACC) exhibits profound therapeutic heterogeneity, with therapy resistance heavily influenced by the immunosuppressive tumor microenvironment. The myeloid compartment, particularly tumor-associated macrophages (TAMs), serves as a key mediator of this therapeutic resistance, yet the precise molecular hubs for predicting neoadjuvant chemotherapy (NACT) sensitivity remain insufficiently characterized. ***Objectives:*** This study aims to decipher the myeloid-driven mechanisms of chemoresistance and validate the clinical utility of the chemokine CCL3 as a predictive and prognostic biomarker in LACC patients to optimize personalized treatment strategies. ***Methods:*** We integrated single-cell transcriptomics (GSE236738) from six LACC patients with high-dimensional Weighted Gene Co-expression Network Analysis (hdWGCNA) to identify macrophage-specific functional modules and hub genes. Subsequent retrospective clinical validation was conducted via immunohistochemistry (IHC) on pre-treatment primary tumor biopsies from a cohort of 33 LACC patients receiving NACT, correlating CCL3 protein expression with RECIST outcomes and survival trajectories. ***Measurements and Main Results:*** Single-cell analysis revealed a substantial expansion of macrophages, accounting for approximately 35% of the immune infiltrate. hdWGCNA pinpointed the chemokine CCL3 as the central hub gene driving this macrophage functional polarization. In the clinical cohort, elevated CCL3 expression was significantly linked to diminished chemosensitivity and a poor pathological response, characterized by higher median Tumor regression rate (based on RECIST 1.1)s (0.31 vs. 0.57; $P = 0.001$). Furthermore, univariate Cox regression and Kaplan-Meier analyses confirmed that high CCL3 expression shows potential as a reliable prognostic factor for both reduced progression-free survival (HR = 1.190; $P = 0.004$) and overall survival (HR = 1.278; $P < 0.001$). ***Conclusions:*** CCL3 is a pivotal orchestrator of macrophage-mediated immune exclusion and chemoresistance in LACC. Assessing CCL3 expression levels provides a promising predictive tool for NACT sensitivity and a vital prognostic indicator, offering actionable insights for developing targeted immunotherapies and advancing precision oncology for LACC management.

Keywords: cervical cancer, CCL3, immunohistochemistry, neoadjuvant chemotherapy, prognosis

1. Introduction

Locally advanced cervical cancer (LACC) constitutes approximately 37% of all cervical carcinoma cases globally (Roberta Massobrio *et al.*, 2024; Carlo Ronsini *et al.*, 2024) and continues to pose a significant major clinical challenge due to its high propensity for recurrence and distant metastasis. Although definitive concurrent

chemoradiotherapy (CCRT) is established as the gold standard of care (Roberta Massobrio *et al.*, 2024; Carlo Ronsini *et al.*, 2024), neoadjuvant chemotherapy (NACT) is increasingly utilized as a strategic intervention to reduce tumor volume, improve operability, and eradicate occult micrometastases (Patricia Pautier, 2024; Malede Birara, Tadesse Urgie & Abraham Fessehaye Sium, 2024; Liang-Chih Liu *et al.*, 2024; Sudeep Gupta *et al.*, 2023; Vanita Noronha *et al.*, 2023; Mei Feng *et al.*, 2023; Young Ju Suh *et al*., 2025; Zi-Tong Zhang *et al.*, 2024; Jing Li *et al.*, 2023; Jing Chen *et al.*, 2023; Hitomi Sakaguchi-Mukaida *et al*., 2023). High-level clinical evidence, notably from the INTERLACE trial, indicates that induction chemotherapy prior to standard CCRT provides significant survival advantages, particularly when utilizing dose-dense weekly platinum-paclitaxel regimens (Mary McCormack *et al.*, 2024; Matheus de Oliveira Andrade *et al.*, 2025). The therapeutic landscape is further evolving with the introduction of neoadjuvant chemo-immunotherapy, which has demonstrated objective response rates as high as 98%, suggesting a powerful synergistic effect in enhancing clinical outcomes (Chen, Z. *et al.*, 2024). Despite these advancements, a striking heterogeneity in therapeutic response persists among LACC patients; for example, while approximately 72.4% of patients may achieve a good pathological response, a significant minority experiences poor outcomes and disease progression (Lijun Wei *et al.*, 2024). This efficacy variance is closely linked to the diverse immune landscapes within the tumor microenvironment and specific clinical-pathological factors such as baseline tumor size and histological grade (Lijun Wei *et al.*, 2024; Antonino Ditto *et al.*, 2024). Consequently, while NACT remains a critical life-saving alternative in settings with limited radiotherapy access (Malede Birara, Tadesse Urgie & Abraham Fessehaye Sium, 2024; Irene Alinafe Chidothe-Chisale *et al.*, 2025), identifying reliable molecular biomarkers is essential to pre-emptively determine therapeutic sensitivity and personalize treatment strategies (Pankaj Garg *et al.*, 2024; Wang, Z. *et al.*, 2023).

The tumor microenvironment (TME) is a complex and dynamic ecosystem where the myeloid compartment, particularly tumor-associated macrophages (TAMs), serves as a key mediator of therapeutic resistance (Arian Jahandideh *et al.*, 2023; Belén Toledo *et al.*, 2024; Bartosz Wilczyński *et al.*, 2024). These highly plastic cells frequently undergo polarization towards a pro-tumorigenic M2-like phenotype, which actively dampens anti-tumor immune responses and creates an immunosuppressive niche conducive to tumor survival (Belén Toledo *et al.*, 2024; Zhang, B. *et al.*, 2023; Liu, C. *et al.*, 2025). This M2-mediated resistance is orchestrated through diverse molecular mechanisms, including the secretion of pro-tumor factors and the modulation of drug metabolism, which collectively shield malignant cells from cytotoxic agents (Belén Toledo *et al.*, 2024; Liu, C. *et al.*, 2025). Furthermore, intercellular communication via extracellular vesicles and cytokines between TAMs and other stromal components facilitates the transport of drug efflux pumps and signaling molecules that enhance chemoresistance (Bartosz Wilczyński *et al.*, 2024). Recent evidence also highlights the role of specific macrophage subsets, such as C1q-expressing populations, in fostering resistance to modern therapies and promoting disease relapse (Caleb K. Stein *et al.*, 2024). Beyond direct biochemical interference, TAMs significantly impact treatment outcomes by promoting angiogenesis and remodeling the extracellular matrix, which can physically impair drug penetration into the tumor core (Arian Jahandideh *et al.*, 2023; Belén Toledo *et al.*, 2024). Consequently, reprogramming the myeloid landscape to favor anti-tumor M1 phenotypes represents a promising strategy to overcome these immunosuppressive barriers and restore therapeutic sensitivity in solid tumors (Zhou, S. *et al.*, 2025).

Among the myriad signaling molecules regulating this myeloid landscape, chemokine (C-C motif) ligand 3 (CCL3) has emerged as a key mediator of macrophage recruitment and functional polarization. Recent evidence underscores the diverse and context-dependent roles of CCL3 across various malignancies (Wang, Z. *et al.*, 2023; Zhou, S. *et al.*, 2025). For instance, in esophageal squamous cell carcinoma, radiotherapy induces CCL3 expression in infiltrating myeloid cells, driving a transition toward a pro-tumorigenic environment (Bryan Chee-chad Lung *et al.*, 2025). Similarly, dysbiosis-induced activation of the CCL3-CCR1 axis has been shown to foster immune evasion and correlates with poor overall survival (Teizo Yoshimura *et al.*, 2023), while myeloid-derived CCL3 recruits CCR1-high monocytes to establish robust immunosuppression under hyperglycemic conditions (Teizo Yoshimura *et al.*, 2023). Conversely, CCL3 can also exhibit anti-tumor properties by triggering pro-inflammatory M1-type polarization, thereby enhancing antigen presentation and the efficacy of both immune checkpoint blockade and chemotherapeutic agents like docetaxel (Yue, S. et al., 2023). Despite its recognized immunomodulatory roles, the specific impact of macrophage-derived CCL3 on NACT resistance in LACC remains poorly understood. To bridge this gap, we first integrated single-cell transcriptomics with high-dimensional network analysis to objectively identify key molecular hubs driving macrophage-mediated chemoresistance. Having pinpointed CCL3 as a central orchestrator in non-responding tumors, we subsequently validated its predictive and prognostic value in a clinical cohort of LACC patients receiving NACT. Ultimately, this study aims to establish CCL3 as a reliable biomarker to guide personalized precision oncology in cervical cancer.

2. Materials and Methods

2.1 Bioinformatics Analysis and Target Identification

Single-cell transcriptomic profiles of tumor samples from six cervical cancer patients (GSE236738) were analyzed using the Seurat package (v4.3.0) (Xiao Liang *et al.*, 2023; Juok Cho *et al.*, 2024; Qiqing Fu *et al.*, 2024; Yu Zhou *et al.*, 2024; Annekathrin Silvia Nedwed *et al.*, 2023). Quality control was performed by excluding cells with nFeature_RNA > 5,000 and a mitochondrial gene proportion (percent.mt) > 10%. After SCTransform normalization, the top 1,500 highly variable genes were selected for Principal Component Analysis (PCA). Batch effects across samples were mitigated using the Harmony algorithm (Sindri Emmanúel Antonsson & Páll Melsted, 2025; John Arévalo *et al.*, 2024). Unsupervised clustering was executed at a resolution of 1.0 using FindNeighbors and FindClusters functions. Cell clusters were visualized via UMAP dimensionality reduction and annotated based on canonical lineage markers. Differential expression patterns between chemo-responsive and non-responsive groups were evaluated using the Wilcoxon rank-sum test.

High-dimensional Weighted Gene Co-expression Network Analysis (hdWGCNA, v0.4.08) was applied to the processed single-cell data (Morabito, S. *et al.*, 2023). The analysis included genes expressed in at least 5% of the total cells. For the macrophage population, a co-expression network was constructed using an optimal soft-thresholding power of 16 (Mahsa Eshaghi & Sajad Rashidi Monfared, 2024; Jing Sui et al., 2025; Muhammad Farhan et al., 2025; Zahra Zinati & Leyla Nazari, 2024; Stephanie P. Klein et al., 2024). Gene modules were identified via hierarchical clustering and the dynamic tree-cut algorithm, visualized through dendrograms. Correlation analysis between gene modules and macrophage identity was conducted to pinpoint key modules. Intramodular connectivity was further calculated to identify central hub genes within these modules.

2.2 Patient Selection and Clinical Cohort

Clinical records of 33 patients with locally advanced cervical cancer (LACC) who received neoadjuvant chemotherapy (NACT) at Renmin Hospital of Wuhan University and Zhongnan Hospital of Wuhan University between 2021 and 2023 were retrospectively reviewed. The cohort comprised 33 female patients with ages ranging from 34 to 75 years. Significant therapeutic response was quantitatively assessed by the tumor regression rate, defined as the percentage decrease in the sum of the longest diameters of target lesions post-NACT compared to baseline, in accordance with RECIST 1.1 guidelines (Zhi-Hua Shi, 2022).

Inclusion criteria were: (1) primary squamous cell carcinoma of the cervix with a maximum tumor diameter > 4 cm; (2) administration of the NACT protocol (2-week Paclitaxel and Platinum-based regimen); (3) availability of comprehensive clinicopathological data. Exclusion criteria included patients with multiple primary malignancies or secondary cervical involvement originating from other metastatic sites. The study protocol was approved by the Medical Ethics Committee of the Medical College of Wuhan University (No: WHU2021-jchx001). Written informed consent for the academic use of clinical data and tissue samples was obtained from all participants prior to their inclusion in the study.

2.3 Immunohistochemistry (IHC) Staining

Immunohistochemical staining was performed to evaluate CCL3 expression in pre-treatment primary tumor biopsy specimens from patients with locally advanced cervical cancer (LACC). Tissue samples were fixed in 4% paraformaldehyde and embedded in paraffin. Serial sections were cut at a thickness of 3–4 μm, baked, deparaffinized, and rehydrated through graded alcohols. Heat-induced epitope retrieval (HIER) was executed in Tris-EDTA buffer (pH 9.0). Slides were then incubated with primary antibody (anti-CCL3, Affinity, DF8572; 1:100 dilution) for 60 minutes. A prediluted horseradish peroxidase (HRP)-conjugated goat anti-rabbit IgG polyclonal antibody was employed as the secondary antibody. The procedure was carried out strictly according to the manufacturer's instructions. Visualization was achieved using 3,3'-diaminobenzidine (DAB), followed by counterstaining with Mayer's hematoxylin.

2.4 Evaluation of IHC Staining

Immunohistochemical (IHC) slides were independently reviewed by two senior pathologists blinded to the clinical outcomes. The expression of CCL3 within the peritumoral stroma was assessed using a semi-quantitative scoring system based on both staining intensity and the percentage of positive cells. The proportion of positive cells was scored as: 0 (<5%), 1 (5%–25%), 2 (26%–50%), 3 (51%–75%), and 4 (>75%). Staining intensity was categorized as: 0 (no staining), 1 (light yellow), 2 (brownish-yellow), and 3 (dark brown). The total IHC score was evaluated by multiplying the staining intensity score (0–3) by the percentage of positive cells score (0–4), resulting in a final score ranging from 0 to 12. For all subsequent statistical analyses, patients were dichotomized into two groups based on the median total score (median = 1.0). Specifically, a total score of ≤ 1 was defined as low CCL3 expression (n = 18), and a total score > 1 was defined as high CCL3 expression (n = 15).

2.5 Patient Follow-up and Survival Definitions

The 33 patients were followed up through a combination of clinical record reviews and telephone interviews. The follow-up period spanned from December 1, 2021, to March 5, 2026, with a median follow-up duration of

35.3 months. Progression-free survival (PFS) was defined as the interval from the initiation of neoadjuvant chemotherapy (NACT) to either the first documentation of disease progression or the date of the last follow-up. Overall survival (OS) was calculated as the time from NACT initiation to death from any cause or the last follow-up.

2.6 Statistical Analysis

Bioinformatics was performed using R (v4.5.0), while clinical data were analyzed via Python (v3.14.0). Survival analysis, including Kaplan-Meier survival curves and Cox proportional hazards regression models, was conducted using the lifelines package (version 0.27.1). Continuous variables were assessed for normality using the Shapiro-Wilk test and compared using independent t-tests or Mann-Whitney U tests. Categorical data were analyzed using Chi-square or Fisher's exact tests. Survival curves for PFS and OS were estimated by the Kaplan-Meier method and compared via log-rank tests. Significant prognostic factors were identified using univariate and multivariate Cox proportional hazards regression models. A two-tailed $P < 0.05$ was considered statistically significant.

3. Results

3.1 Single-Cell Landscape of Cervical Cancer Tissues

To elucidate the cellular determinants of therapeutic efficacy, we characterized the single-cell transcriptional landscapes of patients stratified by their response to NACT. Initial quality control assessments confirmed high data fidelity across all samples, characterized by consistent gene detection frequencies and minimal mitochondrial contamination (Figure 1A-B). Unsupervised clustering partitioned the integrated dataset into 18 distinct clusters (Figure 1C), which were subsequently annotated into nine major cell lineages—including macrophages, epithelial/tumor cells, and various stromal and lymphoid populations (Figure 1D). This annotation was based on the expression of canonical markers, such as TREM2 and APOE for macrophages, and EPCAM and KRT19 for tumor cells (Figure 1E). Quantitative compositional analysis revealed a distinct divergence in the tumor microenvironment (TME) between the two groups. Specifically, non-responding samples were characterized by an extensive presence of tumor cells and a concomitant expansion of the macrophage compartment, which accounted for approximately 35% of the immune infiltrate (Figure 1F). In contrast, responding patients exhibited a higher prevalence of endothelial cells and tumor-infiltrating T and NK cells. The marked accumulation of TREM2+/APOE+ macrophages in non-responders suggests that a polarized, pro-tumorigenic niche contributes to therapeutic resistance, underscoring the potential role of myeloid-driven immune exclusion in dictating clinical outcomes.

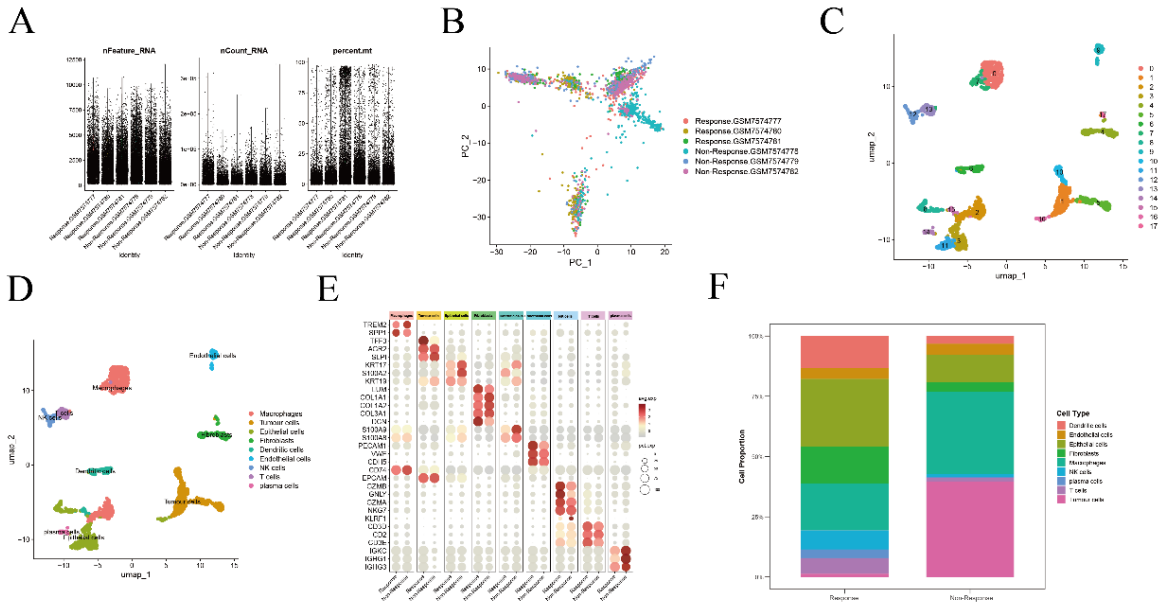

Figure 1. Single-cell Transcriptomic Landscape of Clinical Samples Categorized by Therapeutic Response

(A) Quality control metrics across all sequenced samples, including the number of detected genes (nFeature_RNA), total UMI counts (nCount_RNA), and the percentage of mitochondrial gene expression (percent.mt).

(B) Principal Component Analysis (PCA) plot demonstrating the effective integration of samples from both Response and Non-Response groups, indicating the absence of significant batch effects.

(C) UMAP visualization of 18 transcriptionally distinct cell clusters (Clusters 0–17) identified by unsupervised clustering.

(D) UMAP plot annotated by nine major cell lineages, including Epithelial/Tumor cells, Macrophages, T cells, NK cells, and Fibroblasts.

(E) Dot plot showing the expression of canonical marker genes used for lineage annotation (e.g., EPCAM/KRT19 for tumor cells, TREM2/APOE for macrophages, and CD3D/GZMB for lymphoid cells). The color intensity represents the average expression level, and the dot size indicates the percentage of cells expressing the marker.

(F) Bar plot quantifying the cellular proportions within the tumor microenvironment (TME) of Response and Non-Response groups, highlighting the enrichment of lymphoid populations in responders and tumor cells in non-responders.

3.2 Identification of Macrophage-Specific Hub Modules and CCL3 via hdWGCNA

To further delineate macrophage functional polarization, we applied hdWGCNA and identified 11 co-expression modules under a scale-free topology (R-squared > 0.8, soft-power = 16) (Figure 2A-C). Specificity scoring highlighted the M7 module as a key functional unit highly enriched within the macrophage compartment (Figure 2D-F). Within this regulatory network, the chemokine CCL3 emerged as a central hub gene, with its expression predominantly localized to the macrophage and NK cell lineages (Figure 3A-C). Notably, comparative analysis demonstrated that CCL3 expression was significantly elevated in macrophages derived from the non-response group compared to those from responders ($P < 0.05$; Figure 3D). These findings indicate that the macrophage-derived CCL3 axis may foster an immunosuppressive microenvironment that blunts therapeutic efficacy, positioning it as a key candidate driving treatment resistance.

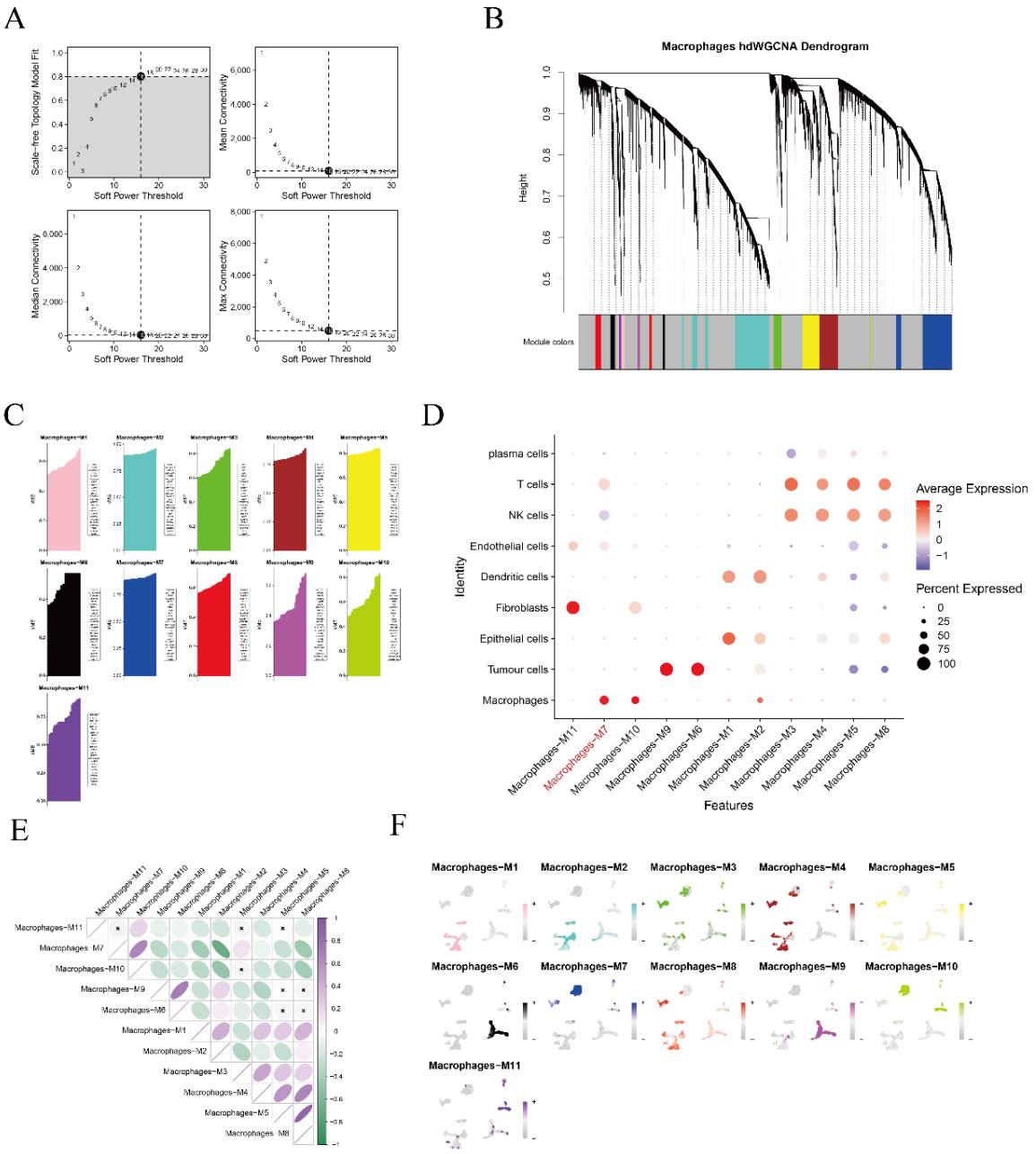

Figure 2. Modular Analysis of Macrophage Heterogeneity via High-Dimensional WGCNA (hdWGCNA)

(A) Selection of the soft-power threshold for network construction. Left: Scale-free topology model fit index (R-squared) as a function of soft-power (Power = 16 achieved R-squared > 0.8). Right: Mean connectivity across various soft-power thresholds.

(B) Gene dendrogram obtained by average linkage hierarchical clustering, with colors representing 11 identified co-expression modules (M1–M11).

(C) Distribution of module eigengenes (MEs) across individual cells within the macrophage compartment.

(D) Dot plot illustrating the specificity of the 11 modules across different cell lineages, identifying M7 as a macrophage-specific functional unit.

(E) Correlation heatmap showcasing the expression relationships and synergies among the identified co-expression modules.

(F) UMAP feature plots projecting the module scores of M1 through M11 onto the macrophage subpopulation, visualizing the spatial distribution of functional modules.

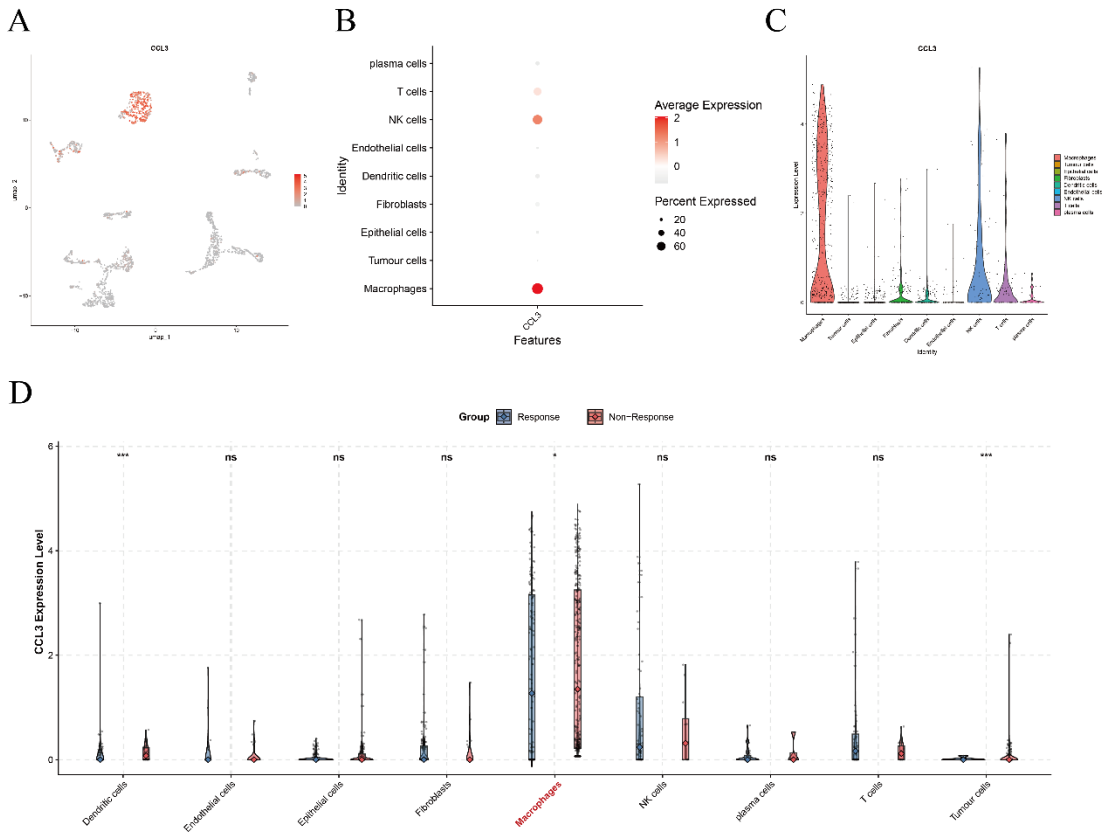

Figure 3. Identification of CCL3 as a Key Hub Gene Associated with Therapeutic Resistance

(A) UMAP feature plot visualizing the expression pattern of CCL3 across the entire single-cell dataset.

(B) Dot plot showing the expression frequency and intensity of CCL3 across major cell types, indicating its predominant origin from Macrophages and NK cells.

(C) Violin plot comparing the transcript levels of CCL3 among various cell lineages.

(D) Comparative analysis of CCL3 expression between Response (blue) and Non-Response (red) groups across identified cell types. Statistical significance was determined by the Wilcoxon rank-sum test (* $p < 0.05$, *** $p < 0.001$, ns: not significant). Note the significant upregulation of CCL3 in macrophages and tumor cells from the non-response cohort.

3.3 Validation of CCL3 Expression in LACC via Immunohistochemistry

To evaluate the clinical relevance of CCL3 in locally advanced cervical cancer (LACC), we performed immunohistochemical (IHC) profiling on 33 patient specimens. CCL3 protein was predominantly localized within the cytoplasm and the surrounding extracellular matrix, exhibiting a distinct expression gradient across the cohort (Figure 4). Quantitative assessment revealed that 36.4% of cases (n = 12) were negative (score 0), 45.5% (n = 15) were weakly positive (score 1–4), and 18.2% (n = 6) exhibited moderate-to-strong positivity (score ≥ 5). Following semi-quantitative scoring that integrated staining intensity and the percentage of positive cells, patients were stratified — based on the median total score (median = 1.0) — into a low-expression group (total score ≤ 1; n = 18, 54.5%) and a high-expression group (total score > 1; n = 15, 45.5%). This stratification served as the primary histological framework for correlating CCL3 abundance with therapeutic outcomes.

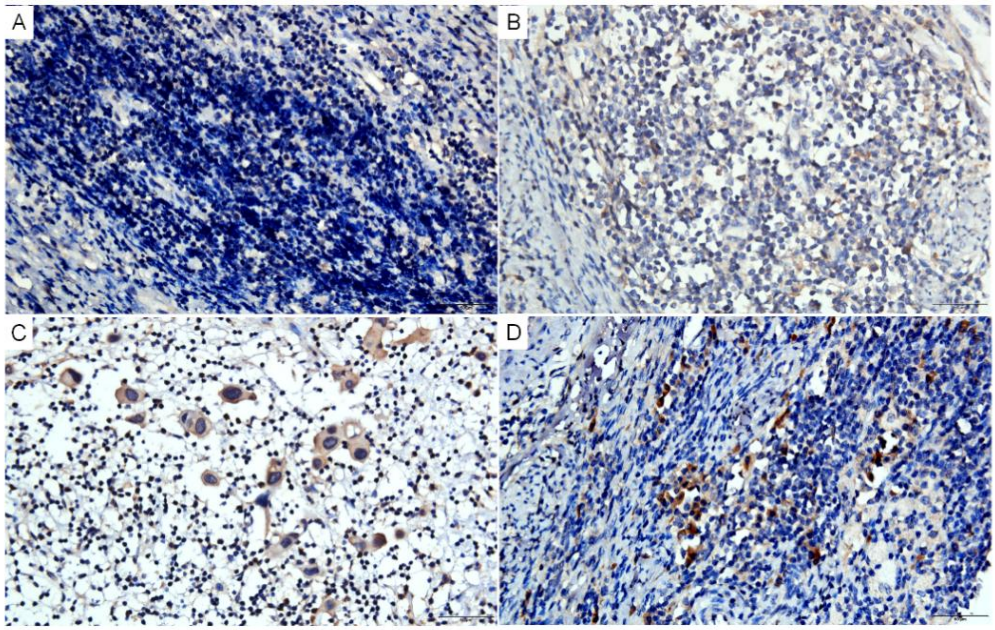

Figure 4. Immunohistochemical (IHC) characterization of CCL3 expression levels in LACC

(A-D) Representative images illustrating the CCL3 staining gradient: (A) negative (score 0), (B) weak (scores 1-4), (C) moderate (scores 5-8), and (D) strong (scores ≥ 9) positivity

Immunoreactivity is primarily concentrated in the cytoplasm. All slides were independently scored by two senior pathologists blinded to clinical data. Patients were dichotomized into low-expression (total score ≤ 1, n = 18) and high-expression (total score > 1, n = 15) cohorts based on the median IHC score. Scale bars = 50 μm.

3.4 Association of CCL3 with Clinicopathological Features and NACT Sensitivity

Analysis of the 33-patient locally advanced cervical cancer cohort established strong comparability between the good response and poor response groups, as baseline parameters—including mean age (57.03 ± 9.25 years) and FIGO stage (60.6% IIA2)—exhibited no statistical divergence (P > 0.05). While aggressive histological features such as nerve and vascular invasion were more frequent in non-responders (35.7% vs. 21.1%), these trends remained statistically non-significant (P = 0.442). Crucially, categorical stratification revealed a robust association between CCL3 levels and treatment efficacy, which was further corroborated by quantitative tumor regression metrics. Specifically, the CCL3-high cohort achieved a significantly lower median Tumor regression rate (based on RECIST 1.1) of 0.31 (IQR: 0.25–0.40) compared to 0.57 (IQR: 0.44–0.62) in the CCL3-low cohort (P = 0.001), indicating that elevated CCL3 levels in the tumor microenvironment are strongly linked to diminished chemosensitivity and a poor pathological response to NACT. Table 2 details the comparison between CCL3-low (n=18) and CCL3-high (n=15) patients, focusing on the substantial divergence in median Tumor regression rate (based on RECIST 1.1)s as a reliable metric for treatment sensitivity (Zhi-Hua Shi, 2022).

Table 1. Clinical characteristics and treatment outcomes of patients according to NACT response

Characteristics	Overall (n=33)	Good response (n=19)	Poor response (n=14)	P value
Age (years, mean ± SD)	57.03 ± 9.25	57.21 ± 10.88	56.79 ± 6.83	0.892
FIGO, No. (%)				
IB3	1 (3.0)	0 (0.0)	1 (7.1)	
IIA	7 (21.2)	3 (15.8)	4 (28.6)	0.139
IIA1	2 (6.1)	2 (10.5)	0 (0.0)	
IIA2	20 (60.6)	14 (73.7)	6 (42.9)	
IIB	3 (9.1)	0 (0.0)	3 (21.4)	
Nerve Invasion, No. (%)				0.442
Positive	9 (27.3)	4 (21.1)	5 (35.7)	

Negative	24 (72.7)	15 (78.9)	9 (64.3)	
Vascular Invasion, No. (%)				
Positive	9 (27.3)	4 (21.1)	5 (35.7)	0.442
Negative	24 (72.7)	15 (78.9)	9 (64.3)	
CCL3 Scores, median (IQR)				
Positive Cell Score	1.0 (0.0–2.0)	1.0 (0.0–2.5)	1.0 (0.0–2.0)	0.812
Intensity Score	2.0 (1.0–2.0)	2.0 (1.0–2.0)	2.0 (1.0–2.0)	0.724
Total Score	5.0 (2.0–8.0)	3.0 (1.0–4.0)	8.0 (5.0–10.0)	0.003
CCL3 Expression, No. (%)				
Low	18 (54.5)	7 (36.8)	11 (78.6)	**0.047**
High	15 (45.5)	12 (63.2)	3 (21.4)	

Note. Data are expressed as mean ± SD, median (IQR), or n (%). P values were calculated using Student's t-test, Mann-Whitney U test, Chi-square test, or Fisher's exact test, as appropriate. Good response: CR or PR; Poor response: SD or PD. CCL3 expression was dichotomized into low (total score ≤ 1) and high (total score > 1) groups based on the median IHC score. Bold P value indicates statistical significance ($P < 0.05$). Abbreviations: NACT, neoadjuvant chemotherapy; FIGO, International Federation of Gynecology and Obstetrics; IQR, interquartile range; SD, standard deviation; RECIST, Response Evaluation Criteria in Solid Tumors; CR, complete response; PR, partial response; CCL3, C-C motif chemokine ligand 3.

Table 2. Association of CCL3 expression with pathological characteristics in locally advanced cervical cancer

Characteristics	n (%)	CCL3 Expression		P value
		CCL3-High (n=15)	CCL3-Low (n=18)	
Age (years)				
< 60 years	22 (66.7)	8	14	0.162
≥ 60 years	11 (33.3)	7	4	
Clinical Stage				
IB/IIA	29 (87.9)	13	16	>0.999
IIB	4 (12.1)	2	2	
Nerve Invasion				
No	22 (66.7)	9	13	0.710
Yes	11 (33.3)	6	5	
Vascular Invasion				
No	23 (69.7)	9	14	0.447
Yes	10 (30.3)	6	4	
Treatment Regimen				
TP	29 (87.9)	13	16	
TP + Immunotherapy	2 (6.1)	2	0	0.253
TC	1 (3.0)	0	1	
LP+CDDP+Nida	1 (3.0)	0	1	
Tumor regression rate (based on RECIST 1.1) [Median (IQR)]	0.41 (0.26–0.58)	0.31 (0.25–0.40)	0.57 (0.44–0.62)	**0.001**

Note. CCL3 expression was dichotomized into low (total score ≤ 1) and high (total score > 1) groups based on the median IHC score. Clinical stage was determined according to FIGO 2018 criteria. Categorical data are presented as n (%), and continuous data as median (interquartile range [IQR]). P values were calculated using Fisher's exact test, Pearson chi-square test, or Mann-Whitney U test, as appropriate. Two-tailed $P < 0.05$ was considered statistically significant.

Abbreviations: FIGO, International Federation of Gynecology and Obstetrics; IQR, interquartile range; LP+CDDP+Nida, lobaplatin + cisplatin + nidaplatin; RECIST, Response Evaluation Criteria in Solid Tumors; TC, taxol + carboplatin; TP, taxol + cisplatin.

3.5 Prognostic Significance of CCL3 for Survival Outcomes in LACC Patients

To elucidate the impact of macrophage heterogeneity on therapeutic response, we constructed gene co-expression networks using hdWGCNA within the macrophage compartment. Applying a soft-threshold power of 16 to achieve a scale-free topology fit (R-squared > 0.8), we identified 11 distinct modules, among which M7 exhibited high macrophage specificity. The chemokine CCL3 emerged as a central hub gene within this regulatory network, with single-cell analysis localizing its expression primarily to macrophages and NK cells. We subsequently validated the clinical utility of CCL3 in a cohort of 33 patients with locally advanced cervical cancer (LACC) using immunohistochemistry. Categorical stratification revealed that high CCL3 expression was significantly enriched in the poor response group compared to good responders (P = 0.047). Crucially, longitudinal Kaplan-Meier survival analysis demonstrated inferior clinical outcomes for patients with elevated CCL3 levels, who exhibited significantly reduced overall survival (OS, P = 0.030) and progression-free survival (PFS, P = 0.004) compared to the low-expression cohort (Figure 5A-B). Collectively, these findings establish CCL3 as a promising predictive biomarker for NACT sensitivity in LACC management. Table 1 summarizes clinical characteristics stratified by NACT response, while Table 2 details the pathological outcomes based on CCL3 status. Representative IHC gradients are shown in Figure 4.

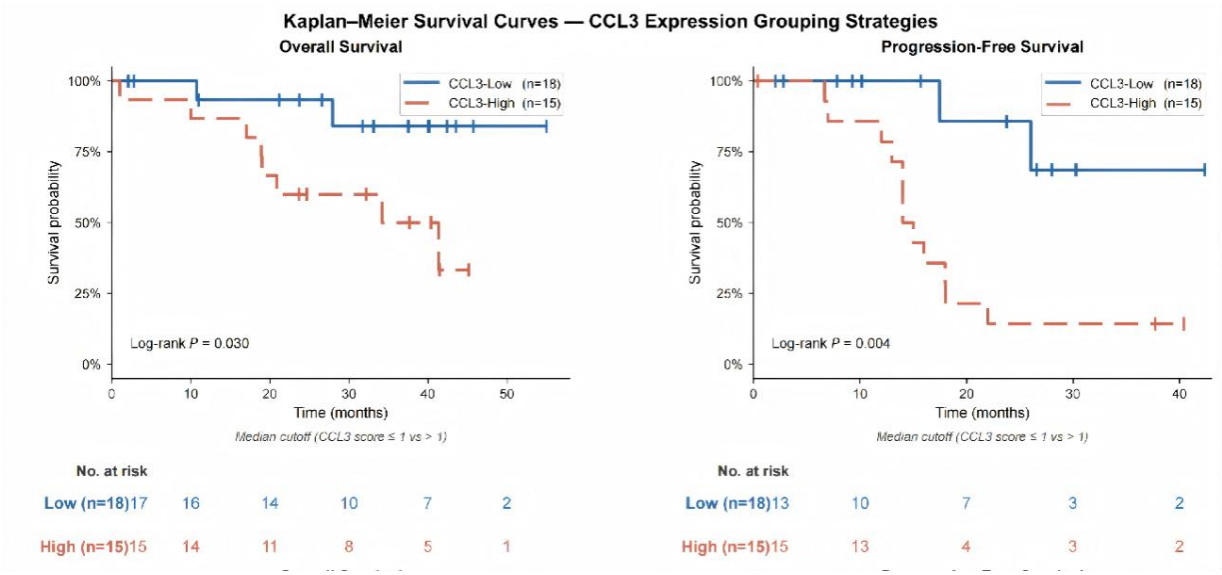

Figure 5. Kaplan-Meier survival analysis of patients stratified by high (total score > 1) versus low (total score ≤ 1) CCL3 expression

Note: (A) Overall survival (OS); (B) Progression-free survival (PFS).

Univariate Cox proportional hazards regression was performed to evaluate the prognostic impact of clinicopathological and molecular variables on progression-free survival (PFS) and overall survival (OS) in this cohort. As detailed in Table 3, conventional clinical parameters, including age, FIGO stage, nerve invasion, and vascular invasion, did not emerge as statistically significant predictors for either survival endpoint (P > 0.05). In contrast, clinical response indicators demonstrated robust prognostic value; a favorable treatment response was strongly associated with a diminished risk of progression (HR = 0.167, P = 0.002) and death (HR = 0.073, P < 0.001). Similarly, the Tumor regression rate (based on RECIST 1.1) served as a significant protective factor for both PFS (P = 0.007) and OS (P = 0.017). Notably, the CCL3 expression score was identified as a significant risk factor for poor prognosis. Higher CCL3 expression levels correlated significantly with an increased hazard of disease progression (HR = 1.190, 95% CI: 1.056–1.342, P = 0.004) and mortality (HR = 1.278, 95% CI: 1.112–1.470, P < 0.001). These findings suggest that while standard pathological features may have limited discriminatory power in this specific cohort, treatment-related responses and CCL3 expression levels offer substantial utility in the risk stratification of LACC patients.

Table 3. Univariate Cox Proportional Hazards Analysis of Prognostic Factors for PFS and OS in 33 Patients with Locally Advanced Cervical Cancer

Variable	PFS		OS	
	HR (95% CI)	P value	HR (95% CI)	P value
Age (years)	1.016 (0.955–1.081)	0.612	1.075 (0.991–1.167)	0.082
FIGO	0.474 (0.104–2.149)	0.333	0.684 (0.085–5.474)	0.720
Nerve Invasion	1.393 (0.456–4.258)	0.561	0.643 (0.166–2.493)	0.523
Vascular Invasion	1.357 (0.454–4.058)	0.585	1.156 (0.324–4.125)	0.823
Treatment Response	0.167 (0.052–0.531)	0.002	0.073 (0.018–0.304)	< 0.001
Tumor regression rate (based on RECIST 1.1)	0.012 (0.000–0.297)	0.007	0.030 (0.002–0.530)	0.017
CCL3 Expression Score	1.190 (1.056–1.342)	0.004	1.278 (1.112–1.470)	< 0.001

Abbreviations: HR, hazard ratio; CI, confidence interval; PFS, progression-free survival; OS, overall survival; MRI, magnetic resonance imaging; RECIST, Response Evaluation Criteria In Solid Tumours; CR, complete response; PR, partial response; SD, stable disease; PD, progressive disease; TP, taxol + cisplatin. CCL3 High Expression defined as CCL3 Total Score > 1 (median, n = 15); CCL3 Low Expression: Score ≤ 1 (n = 18). Significant P values (< 0.05) shown in bold red. Cox proportional hazards model; HR > 1 indicates worse prognosis.

4. Discussion

The profound heterogeneity of the tumor immune microenvironment in locally advanced cervical cancer (LACC) remains a primary barrier to achieving consistent efficacy with neoadjuvant chemotherapy (NACT), frequently leading to variable treatment responses and disease relapse (Mary McCormack *et al.*, 2024; Lijun Wei *et al.*, 2024). While emerging evidence highlights the substantial role of tumor-associated macrophages in orchestrating chemoresistance across various malignancies (Belén Toledo *et al.*, 2024; Bo Yin *et al.*, 2025), precise molecular biomarkers capable of predicting this myeloid-driven resistance in LACC remain clinically elusive. By integrating single-cell transcriptomic profiling with high-dimensional weighted gene co-expression network analysis (hdWGCNA), our study identified the chemokine CCL3 as a central hub gene dictating the functional polarization of a distinct macrophage subpopulation. This initial finding was strictly substantiated in a reliable clinical validation cohort. Immunohistochemical assessments revealed that elevated CCL3 expression within the LACC microenvironment strongly correlates with inferior pathological responses and diminished sensitivity to NACT. Furthermore, longitudinal survival analyses confirmed that a high CCL3 burden serves as a significant prognostic factor for both shortened progression-free and overall survival. Together, these findings establish the clinical utility of CCL3 as a reliable predictive biomarker for treatment resistance and poor prognosis, offering a valuable molecular tool to guide personalized therapeutic interventions targeting the myeloid compartment in cervical cancer.

Our scRNA-seq analysis revealed a striking expansion of the macrophage population, which constituted approximately 35% of the immune infiltrate in the non-responder (NR) group following neoadjuvant chemotherapy. This pronounced accumulation aligns with clinical observations where CD68+ macrophages predominantly populate the tumor microenvironment (TME) of advanced cervical cancer patients failing to respond to standard therapies (Patrícia Rocha Martins *et al.*, 2023). The dramatic influx of macrophages can be attributed to the synergistic interplay between residual tumor cells and chemotherapeutic agents, which actively reshapes the myeloid compartment and promotes the survival and marker expression of M2-like phenotypes (Patrícia Rocha Martins *et al.*, 2023; Viktória Jenei *et al.*, 2025). Within this repopulated landscape, our data highlights a prominent subset of CCL3-expressing macrophages. Although the precise mechanisms of CCL3 in cervical cancer chemoresistance remain underexplored, tumor-associated macrophages (TAMs) are known to establish supportive niches for immune evasion and therapeutic resistance through complex cytokine and chemokine crosstalk (Yue, S. et al., 2023). We hypothesize that these CCL3+ macrophages act as central signaling hubs, secreting chemokines to recruit further immunosuppressive populations and impair T-cell function, mirroring the T-cell exhaustion and reduced cytotoxicity observed in SCCA-mediated macrophage polarization (Chen, Z. *et al.*, 2024). Consequently, this dynamic CCL3-driven network fortifies an immunosuppressive barrier within the TME, directly contributing to the refractory nature and poor prognosis of the NR cohort.

Building on current literature, we hypothesize that the expanded macrophages in the non-responder (NR) microenvironment drive cervical cancer immunosuppression and chemoresistance primarily via CCL3 secretion.

Mechanistically, CCL3 likely engages its receptors, CCR1 or CCR5, to recruit immunosuppressive populations such as regulatory T cells (Tregs) and monocytes into the tumor bed, thereby facilitating immune evasion (Zaineb Hassouneh *et al.*, 2024). Furthermore, the CCL3-CCR1 signaling axis can stabilize direct physical interactions between macrophages and tumor cells, a critical step for promoting metastasis and therapeutic resistance (Teizo Yoshimura *et al.*, 2023). Concurrently, this localized CCL3 overexpression — resembling the CCL3high PD-L1high super-immunosuppressive subsets observed in other malignancies — may exacerbate dysregulated inflammatory responses and subsequently impair the infiltration and cytotoxic efficacy of CD8+ T cells (Jing Li *et al.*, 2023; Liu, C. *et al.*, 2025). Beyond immune modulation, CCL3 might also directly fuel tumor progression by activating downstream epigenetic targets like m6A modifications (Zhou, S. *et al.*, 2025). Therefore, targeting this macrophage-driven CCL3 chemokine network holds promise for dismantling this multidimensional pro-tumorigenic cascade.

Given the critical role of CCL3 in macrophage-mediated chemoresistance, our findings demonstrate substantial clinical translational potential. Because patients with locally advanced cervical cancer exhibit significant heterogeneity in their responses to neoadjuvant chemotherapy (NACT) (Patricia Pautier, 2024), CCL3 emerges as a promising predictive biomarker within the precision medicine framework (Pankaj Garg *et al.*, 2024). Evaluating CCL3 expression and the histological distribution of specific macrophages in pre-treatment biopsies via routine immunohistochemistry (IHC) provides a cost-effective and intuitive method to profile the immunosuppressive microenvironment. For potential non-responders presenting with elevated CCL3 levels, clinicians might bypass standard NACT to prevent ineffective drug toxicity, opting instead for upfront concurrent chemoradiotherapy or alternative strategies involving immunotherapies. Integrating CCL3 assessment into standard pathological screening protocols will strongly facilitate personalized therapeutic stratification, optimize clinical decision-making, and ultimately improve survival benefits in cervical cancer management.

While our findings highlight the critical role of macrophage-derived CCL3 in cervical cancer chemoresistance — suggesting it shows potential as a reliable prognostic factor—certain limitations exist (Viktória Jenei *et al.*, 2025). Primarily, alongside the exploratory retrospective design, we must explicitly acknowledge that the small sample size intrinsically limits the statistical power of our Cox regression analyses. The single-center nature of the data also necessitates cautious interpretation regarding clinical generalizability. As advocated in recent oncology studies (Angela Collarino *et al.*, 2024), future validation across large-sample, multi-center prospective cohorts is strictly required to firmly establish the prognostic value of CCL3. Additionally, deeper mechanistic investigations are necessary to fully elucidate the immunosuppressive microenvironment reprogramming driven by these macrophages, ultimately bridging the gap toward effective clinical translation and personalized therapy. Finally, while our scRNA-seq analysis localized CCL3 expression predominantly to the macrophage compartment, our clinical validation relied on single-plex IHC. Future spatial transcriptomics or multiplex immunofluorescence (e.g., CCL3/CD68 co-staining) studies are warranted to precisely map the cellular origins and spatial interactions of CCL3 within the LACC microenvironment.

Data Availability Statement

The data are available upon reasonable request.

Competing Interests

The authors declare no competing interests.

Ethics Approval and Consent to Participate

This study was approved by the ethical standards of the Medical Ethics Committee of the Medical College of Wuhan University (No: WHU2021-jchx001). Written informed consent for the use of tissue samples in research was obtained from all participants.

Conceptualization

H.C. performed development of methodology and writing, review, revision of the paper, provided acquisition, analysis, and interpretation of data; HL.C. statistical analysis provided technical and material support. All authors read and approved the final paper.

References

Angela Collarino *et al.* (2024). Is PET radiomics useful to predict pathologic tumor response and prognosis in locally advanced cervical cancer? *The Journal of Nuclear Medicine.* https://doi.org/10.2967/jnumed.123.267044

Annekathrin Silvia Nedwed *et al.* (2023). Using combined single-cell gene expression, TCR sequencing and cell

surface protein barcoding to characterize and track CD4+ T cell clones from murine tissues. *Frontiers in Immunology*. doi:10.3389/fimmu.2023.1241283.

Antonino Ditto *et al.* (2024). Are biomarkers expression and clinical-pathological factors predictive markers of the efficacy of neoadjuvant chemotherapy for locally advanced cervical cancer? *Eur J Surg Oncol, 50*, 108311–108311.

Arian Jahandideh *et al.* (2023). Macrophage's role in solid tumors: Two edges of a sword. *Cancer Cell International,* 23.

Bartosz Wilczyński, Alicja Dąbrowska, Julita Kulbacka, & Dagmara Baczyńska. (2024). Chemoresistance and the tumor microenvironment: The critical role of cell–cell communication. *Cell Communication and Signaling, 22*.

Belén Toledo *et al.* (2024). Deciphering the performance of macrophages in tumour microenvironment: a call for precision immunotherapy. *Journal of Hematology & Oncology, 17*.

Bo Yin, Chun Chen, Tiefeng Huang. (2025). Oncogenic CMTM6 drives M2a macrophages formation and fuels cervical cancer progression. *Front Immunol.* doi:10.3389/fimmu.2025.1621816.

Bryan Chee-chad Lung *et al.* (2025). [Conference Abstract] 6135: Characterization of monocytic-myeloid populations in the tumor microenvironment using patient-derived organoid xenograft models and macrophage-depleting therapies in esophageal squamous cell carcinoma. *Cancer Res, 85*, 6135–6135.

Caleb K. Stein *et al.* (2024). Abundance of C1q Expressing Macrophages Promotes Resistance to Modern Therapy. *Blood, 144*, 3275.

Carlo Ronsini *et al.* (2024). Locally Advanced Cervical Cancer: Neoadjuvant Treatment versus Standard Radio-Chemotherapy—An Updated Meta-Analysis. *Cancers, 16*, 2542.

Chen, Z. *et al.* (2024). Deep learning on tertiary lymphoid structures in hematoxylin-eosin predicts cancer prognosis and immunotherapy response. *npj Precis Oncol, 8*, 73.

Hitomi Sakaguchi-Mukaida *et al*. (2023). Systematic Review of the Survival Outcomes of Neoadjuvant Chemotherapy in Women with Malignant Ovarian — An Germ Cell Tumors. *Cancers.* https://doi.org/10.3390/cancers15184470

Irene Alinafe Chidothe-Chisale *et al.* (2025). Outcomes and toxicity profiles of two-drug versus three-drug neoadjuvant chemotherapy for locally advanced cervical cancer in a setting without radiotherapy: Insights from Malawi. *J Clin Oncol, 43*.

Jing Chen *et al.* (2023). Neoadjuvant camrelizumab plus chemotherapy for locally advanced cervical cancer (NACI Study): a study protocol of a prospective, single-arm, phase II trial. *BMJ Open, 13*, e067767–e067767.

Jing Li *et al.* (2023). Neoadjuvant chemotherapy with weekly cisplatin and paclitaxel followed by chemoradiation for locally advanced cervical cancer. *BMC Cancer,* 23.

Jing Sui, Yanni Zhang, Linjie Zhang, Hui Xia. (2025). Identification and Evaluation of Hub Long Non-Coding RNAs and mRNAs in PM2.5-Induced Lung Cell Injury. *International Journal of Molecular Sciences, 26*, 911–911.

John Arévalo *et al.* (2024). Evaluating batch correction methods for image-based cell profiling. *Nature Communications, 15*,

Juok Cho, Bukyung Baik, NULL AUTHOR_ID, Daeui Park, & NULL AUTHOR_ID. (2024). Characterizing efficient feature selection for single-cell expression analysis. *Briefings in Bioinformatics,* 25.

Liang-Chih Liu *et al.* (2024). A proof-of-concept study of LXP5268 as an add-on neoadjuvant chemotherapy in patients with early-stage triple-negative breast cancer. *J Clin Oncol, 42*, e12607.

Lijun Wei *et al.* (2024). Evaluation of pathological response to neoadjuvant chemotherapy in locally advanced cervical cancer. *J Transl Med, 22*, 655.

Liu, C., Huang, J., Cai, P., Jiang, M. & Chen, H. (2025). From COPD to cancer: Indacaterol's unexpected role in combating NSCLC. *Front Pharmacol, 16*, 1579126.

Mahsa Eshaghi & Sajad Rashidi Monfared. (2024). Co-regulatory network analysis of the main secondary metabolite (SM) biosynthesis in Crocus sativus L. *Dental Sci Rep, 14*.

Malede Birara, Tadesse Urgie, Abraham Fessehaye Sium. (2024). Locally advanced cervical cancer: Neoadjuvant chemotherapy plus radical surgery an alternative approach to chemo-radiation in a low-income setting: A descriptive study. *PLoS ONE, 19*, e0310457.

Mary McCormack *et al.* (2024). Induction chemotherapy followed by standard chemoradiotherapy versus standard chemoradiotherapy alone in patients with locally advanced cervical cancer (GCIG INTERLACE): An international, multicentre, randomised phase 3 trial. *Lancet,* 1525.

Matheus de Oliveira Andrade *et al.* (2025). A meta-analysis of induction chemotherapy (ICT) followed by chemoradiotherapy for locally advanced cervical cancer: The role of ICT type and duration on efficacy outcomes. *J Clin Oncol, 43*, 5539.

Mei Feng *et al.* (2023). Low-Dose Fractionated Radiotherapy Combined with Neoadjuvant Chemotherapy for T3-4 Nasopharyngeal Carcinoma Patients: The Preliminary Results of a Phase II Randomized Controlled Trial. *Int J Radiat Oncol Biol Phys, 117*, e580–e581.

Morabito, S., Reese, F., Rahimzadeh, N., Miyoshi, E. Swarup, V. (2023). hdWGCNA identifies co-expression networks in high-dimensional transcriptomics data. *Cell Reports Methods, 3*, 100498.

Muhammad Farhan, Muhammad Ikram, J. Sun, Sanwei Yang, & Yong Wang. (2025). Identification of Leaf Rust-Related Gene Signature in Wheat (Triticum Aestivum L.) Using High-Throughput Sequencing, Network Analysis, and Machine Learning Algorithms. *Rice,* 18.

Pankaj Garg *et al.* (2024). Emerging biomarkers and molecular targets for precision medicine in cervical cancer. *Biochimica Et Biophysica Acta - Reviews On Cancer,* 189106–189106. doi:10.1016/j.bbcan.2024.189106.

Patricia Pautier. (2024). Is there finally a place for neoadjuvant treatment in locally advanced cervical cancer? *Lancet Oncology*. doi:10.1016/s1470-2045(23)00576-4.

Patrícia Rocha Martins *et al.* (2023). Linking tumor immune infiltrate and systemic immune mediators to treatment response and prognosis in advanced cervical cancer. *Sci Rep, 13*.

Qiqing Fu *et al.* (2024). A comparison of scRNA-seq annotation methods based on experimentally labeled immune cell subtype dataset. *Briefings in Bioinformatics,* 25.

Roberta Massobrio *et al.* (2024). New Frontiers in Locally Advanced Cervical Cancer Treatment. *Stomatology, 13*, 4458.

Sindri Emmanúel Antonsson & Páll Melsted. (2025). Batch correction methods used in single-cell RNA sequencing analyses are often poorly calibrated. *Genome Research.* doi:10.1101/gr.279886.124.

Stephanie P. Klein, Shawn M. Kaeppler, Kathleen M. Brown, Jonathan P. Lynch. (2024). Integrating GWAS with a gene co-expression network better prioritizes candidate genes associated with root metaxylem phenes in maize. *The Plant Genome.* https://doi.org/10.1002/tpg2.20489

Sudeep Gupta *et al.* (2023). Abstract GS5-01: Addition of platinum to sequential taxane-anthracycline neoadjuvant chemotherapy in patients with triple-negative breast cancer: A phase III randomized controlled trial. *Cancer Research*.

Teizo Yoshimura, Chunning Li, Yuze Wang, Akihiro Matsukawa. (2023). The chemokine monocyte chemoattractant protein-1/CCL2 is a promoter of breast cancer metastasis. *Cell Mol Immunol, 20*, 714–738.

Vanita Noronha *et al.* (2023). Long-term outcomes of neo-adjuvant chemotherapy on borderline resectable oral cavity cancers: Real-world data of 3266 patients and implications for clinical practice. *Oral Oncol, 148*, 106633.

Viktória Jenei *et al.* (2025). Anthracycline Treatments and the Presence of Tumor Cells Synergistically Modify the Composition of Macrophage Subpopulations in the Co-Culture System. *Int J Mol Sci, 26*, 9202.

Wang, Z. *et al.* (2023). An immune cell atlas reveals the dynamics of human macrophage specification during prenatal development. *Cell, 186*, 4454-4471.e19.

Xiao Liang *et al.* (2023). A critical assessment of clustering algorithms to improve cell clustering and identification in single-cell transcriptome study. *Briefings in Bioinformatics, 25*.

Young Ju Suh, Dae-Hyung Lee, Hee Joong Lee, Banghyun Lee. (2025). Neoadjuvant Chemotherapy Followed by Concurrent Chemoradiation Versus Adjuvant Chemotherapy Following Concurrent Chemoradiation for Locally Advanced Cervical Cancer: A Network Meta-Analysis. *Cancers, 17*, 223.

Yu Zhou *et al.* (2024). Prognostic prediction using a gene signature developed based on exhausted T cells for liver cancer patients. *Heliyon*. doi:10.1016/j.heliyon.2024.e28156.

Yue, S., Wang, Q., Zhang, J., Hu, Q. & Liu, C. (2023). Understanding cervical cancer at single-cell resolution. *Cancer Lett, 576*, 216408.

Zahra Zinati, Leyla Nazari. (2024). Population-specific gene expression profiles in prostate cancer: Insights from weighted gene co-expression network analysis (WGCNA). *World J Surg Oncol, 22*.

Zaineb Hassouneh *et al.* (2024). The Laws of Attraction: Chemokines as Critical Mediators in Cancer Progression and Immunotherapy Response in Bladder Cancer. *Cancers, 16*, 3303–3303.

Zhang, B. *et al.* (2023). Single-cell chemokine receptor profiles delineate the immune contexture of tertiary lymphoid structures in head and neck squamous cell carcinoma. *Cancer Lett, 558*, 216105.

Zhi-Hua Shi. (2022). Progression-free survival: It is time for a new name. *Lancet Oncology, 23*, 328–330.

Zhou, S. *et al.* (2025). Artificial intelligence in gastrointestinal cancer research: Image learning advances and applications. *Cancer Lett, 614*, 217555.

Zi-Tong Zhang *et al.* (2024). Neoadjuvant chemoradiotherapy versus neoadjuvant chemotherapy for initially unresectable locally advanced colon cancer: short-term outcomes of an open-label, single-centre, randomised, controlled, phase 3 trial. *EClinicalMedicine, 76*, 102836.